JOC Article
pubs.acs.org/joc

Computational Chemical Studies on Thermochemistry and Ring Strains in Cyclic [*n*]Metaphenyleneacetylenes, Butadiyne-Bridged [4$_n$]Metacyclophynes, and Butadiyne-Bridged [4$_n$]Paracyclophynes

Mohamad Akbar Ali and Mangala Sunder Krishnan*

Department of Chemistry, Indian Institute of Technology (IIT) Madras, Chennai 600036, India

mangal@iitm.ac.in

Received March 30, 2010

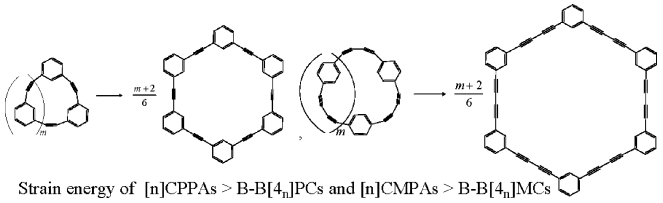

Strain energy of [n]CPPAs > B-B[4$_n$]PCs and [n]CMPAs > B-B[4$_n$]MCs

The thermochemical properties and ring strains in cyclic [*n*]metaphenyleneacetylenes ([*n*]CMPAs), butadiyne-bridged [4$_n$]metacyclophynes (B-B[4$_n$]MCs), and butadiyne-bridged [4$_n$]paracyclophynes (B-B[4$_n$]PCs) were studied using a homodesmotic reaction scheme coupled with density functional theory (B3LYP/6-31G*, mPW1PW91/6-31G*, and M06-2X/6-31+G**//B3LYP/6-31G*). Strain energies of [*n*]CMPAs and B-B[4$_n$]MCs decrease first from very high values for small rings to become zero when *n* becomes 6, then increase with *n*, and finally decrease as *n* becomes larger than 8. In the case of B-B[4$_n$]PCs, strain energies decrease with increasing *n*. Heats of formation of [*n*]CMPAs, B-B[4$_n$]MCs, and B-B[4$_n$]PCs increase steadily with increasing numbers of phenylacetylene and 1-(buta-1,3-diynyl)benzene to reach a near-constant value per unit monomer as *n* increases. The geometries and (vibrational and nuclear magnetic resonance) spectroscopic properties of [*n*]CMPAs, B-B[4$_n$]MCs, and B-B[4$_n$]PCs were also studied. Geometrical parameters, Raman frequencies, and ^{1}H NMR chemical shifts of [3]CMPA and [4]CMPA are found to be in good agreement with compounds for which there are experimentally available values at the B3LYP/6-31G* level of theory. In addition, electronic structure calculations were carried out for [*n*]CMPAs, B-B[4$_n$]MCs, and B-B[4$_n$]PCs. Ring diameters were also calculated for B-B[4$_n$]PCs.

1. Introduction

Considerable developments have happened in the field of supramolecular chemistry during the past decade.[1,2] Conformationally rigid and shape-persistent macrocyclic cyclophynes having acetylenic linkages have attracted a great deal of interest because of their host−guest chemistry,[3] electronic properties,[4] and strain energies[5] and because they are precursors for fullerenes.[6,7] Cyclophanes[8−10] are also important

(1) (a) Schneider, H. J.; Durr, H. *Frontiers in Supramolecular Organic Chemistry and Photochemistry*; VCH: New York, 1991. (b) Gokel, G. W. *Advances in Supramolecular Chemistry*; JAI Press: Greenwich, CT, 1992; Vol. 2. (c) Balzani, V.; De Cola, L. *Supramolecular Chemistry*; Kluwer Academic: Dordrecht, The Netherlands, 1991. (d) van Binst, G. *Design and Synthesis of Organic Molecules Based on Molecular Recognition*; Springer-Verlag: Berlin, 1986.

(2) (a) Lehn, J.-M. *Angew. Chem., Int. Ed. Engl.* **1988**, *27*, 89. *Angew. Chem., Int. Ed. Engl.* **1990**, *29*, 1304. (b) Cram, D. J. *Angew. Chem., Int. Ed. Engl.* **1988**, *27*, 1009. (c) Hong, J.-I.; Feng, Q.; Rotello, V.; Rebek, J., Jr. *Science* **1992**, *255*, 848. (d) Whitesides, G. M.; Mathias, J. P.; Seto, C. T. *Science* **1991**, *254*, 1312. (e) Muehldorf, A. V.; Van Engen, D.; Warner, J. C.; Hamilton, A. D. *J. Chem. Soc.* **1988**, *110*, 6561. (f) Zimmerman, S. C.; Wu, W. *J. Am. Chem. Soc.* **1989**, *111*, 8054.

(3) (a) Tobe, Y.; Utsumi, N.; Nagano, A.; Naemura, K. *Angew. Chem., Int. Ed.* **1998**, *37*, 285. (b) Henze, O.; Lentz, D.; Schluter, A. D. *Chem.—Eur. J.* **2000**, *6*, 2362. (c) Kawase, T.; Hosokawa, Y.; Kurata, H.; Oda, M. *Chem. Lett.* **1999**, *28*, 745. (d) Morrison, D. L.; Hoger, S. *Chem. Commun.* **1996**, 2313.

(4) (a) Kawase, T.; Darabi, H. R.; Oda, M. *Angew. Chem., Int. Ed. Engl.* **1996**, *35*, 2664. (b) Pak, J. J.; Weakley, T. J. R.; Haley, M. M. *J. Am. Chem. Soc.* **1999**, *121*, 8182. (c) Matzger, A. J.; Vollhardt, K. P. C. *Tetrahedron Lett.* **1998**, *39*, 6791.

(5) (a) Kawase, T.; Darabi, H. R. *Chem. Rev.* **2006**, *106*, 5250. (b) Kawase, T.; Ueda, N.; Oda, M. *Tetrahedron Lett.* **1997**, *38*, 6681. (c) Kawase, T.; Ueda, N.; Darabi, H. R.; Oda, M. *Angew. Chem., Int. Ed. Engl.* **1996**, *35*, 1556.

(6) Kawase, T.; Nishiyama, Y.; Nakamura, T.; Ebi, T.; Matsumoto, K.; Kurata, H.; Oda, M. *Angew. Chem., Int. Ed.* **2007**, *46*, 1086.

DOI: 10.1021/jo100603a Published on Web 08/10/2010

in the study of carbon nanotubes. [2.2]Ortho-, [2.2]meta-, and [2.2]paracyclophynes, replacing ethano groups with one or two acetylenic bonds form a novel group of compounds known as cyclic [*n*]orthophenyleneacetylenes ([*n*]COPAs), cyclic [*n*]metaphenyleneacetylenes ([*n*]CMPAs), cyclic [*n*]-paraphenyleneacetylenes ([*n*]CPPAs), butadiyne-bridged [4_n]orthocyclophynes (B-B[4_n]OCs), butadiyne-bridged [4_n]metacyclophynes (B-B[4_n]MCs), and butadiyne-bridged [4_n]paracyclophynes (B-B[4_n]PCs), respectively. There are specific experimental studies on [2]COPAs, [*n*]CMPAs (n = 3−7), [*n*]CPPAs (n = 5−9), B-B[4_n]MCs (n = 3), and their derivatives and methoxy derivatives of B-B[4_n]PCs (n = 2−3).[4−7,11−18] [*n*]CMPAs and B-B[4_n]MCs are molecular models for these kinds of materials and can potentially form various new types of molecular electronic devices[19−23] such as rectifiers,[19,20] memory devices,[21] switches,[22] and transistors.[23] It is important to establish trends in molecular strain with increasing numbers of phenylacetylene and 1-(buta-1,3-diynyl)benzene units. [*n*]CPPAs and B-B[4_n]PCs are model compounds for carbon nanotubes. The strain energies of these macrocycles are found to decrease as the number of phenylacetylene or 1-(buta-1,3-diynyl)benzene units increases. It has been suggested that, because the ring size of the diyne-bridged macrocycles is larger than that of [*n*]CMPAs having the same number of aromatic rings, it is possible to introduce guest binding sites along the interior of the macrocycles.[15] Recently, we have reported the geometries, thermodynamic properties, strain energies, and electronic properties of several [*n*]CPPAs.[24] Itami et al. have reported the strain energies of [*n*]cycloparaphenylenes (n = 6−20) using homodesmotic reactions in combination with the B3LYP/6-31G* level of theory.[25] Here we present a comprehensive account of our studies on [*n*]CMPAs, B-B[4_n]MCs, and B-B[4_n]PCs using density functional theory (B3LYP/6-31G*, mPW1PW91/6-31G*, and M06-2X/6-31+G**//B3LYP/6-31G*) that we hope will be helpful to the experimentalists who design possible synthetic routes to some of these oligomers.

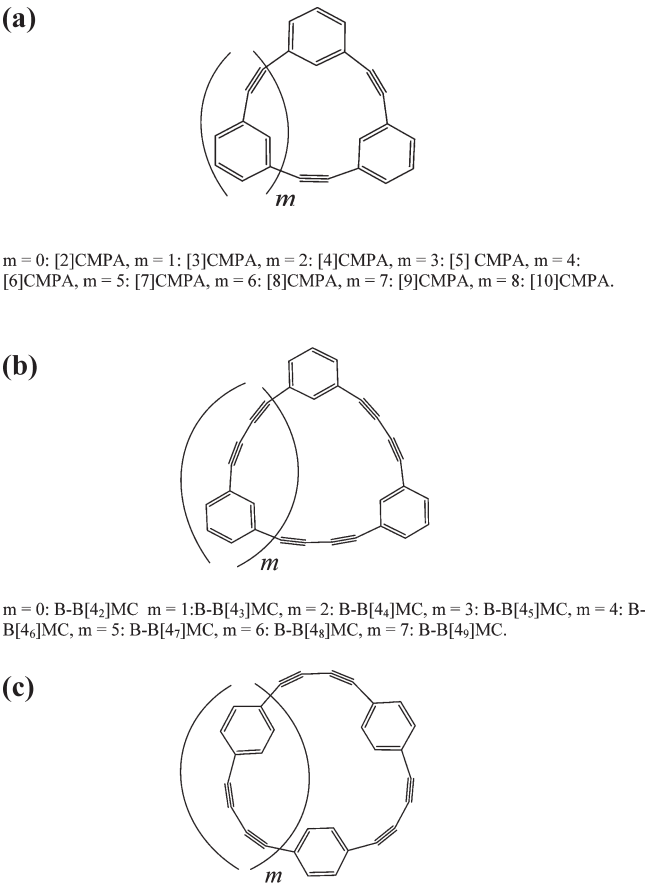

FIGURE 1. Polymeric structure of [*n*]CMPAs, B-B[4_n]MCs, and B-B[4_n]PCs where n (m = n − 2) represents the number of phenylacetylene and 1-(buta-1,3-diynyl)benzene units.

Ring strain energy is a relative quantity. It is the excess energy between cyclic molecules and a chosen strain-free reference system. The idea of strain energies was first put forward by Adolf von Bayer[26] in 1885 for understanding chemical properties. His idea was very useful and accurate for three- and four-membered rings. The group equivalent method, Westheimer bond angle method,[27] Dudev ring fragment method,[28] Wiberg heats of reaction method, isodesmic and homodesmotic reaction approaches, etc.,[8−10,29−31] are a few widely used methods in the literature for calculating the strain energies of cyclic and noncyclic molecules. We have

(7) (a) Rubin, Y.; Parker, T. C.; Khan, S. I.; Holliman, C. L.; McElvany, S. W. *J. Am. Chem. Soc.* **1996**, *118*, 5308. (b) Tobe, Y.; Nakagawa, N.; Naemura, K.; Kishi, J.; Sonoda, M.; Naemura, K.; Wakabayashi, T.; Shida, T.; Achiba, Y. *Tetrahedron* **2001**, *57*, 3629.
(8) Caramori, G. F.; Galembeck, S. E.; Lalli, K. K. *J. Org. Chem.* **2005**, *70*, 3242.
(9) Hong, B. Y.; Lee, J. Y.; Cho, J. S.; Yun, S.; Kim, K. S. *J. Org. Chem.* **1999**, *64*, 5661.
(10) Jarowski, P. D.; Diederich, F.; Houk, K. N. *J. Org. Chem.* **2005**, *70*, 1671.
(11) (a) Haley, M. M.; Brand, S. C.; Pak, J. J. *Angew. Chem., Int. Ed. Engl.* **1997**, *36*, 836. (b) Wan, W. B.; Brand, S. C.; Pak, J. J.; Haley, M. M. *Chem.—Eur. J.* **2000**, *6*, 2044.
(12) For related butadiyne-bridged orthocyclophynes, see: (a) Zhou, Q.; Carroll, P. J.; Swager, T. M. *J. Org. Chem.* **1994**, *59*, 1294. (b) Guo, L.; Bradshaw, J. B.; Tessier, C. A.; Youngs, W. J. *J. Chem. Soc., Chem. Commun.* **1994**, 243.
(13) Kawase, T.; Ueda, N.; Tanaka, K.; Seirai, Y.; Oda, M. *Tetrahedron Lett.* **2001**, *42*, 5509.
(14) Balwin, K. P.; Simons, R. S.; Rose, J.; Zimmerman, P.; Hercules, D. V.; Tessier, C. A.; Youngs, W. J. *J. Chem. Soc., Chem. Commun.* **1994**, 1257.
(15) Tobe, Y.; Utsumi, N.; Nagano, A.; Sonoda, M.; Naemura, K. *Tetrahedron* **2001**, *57*, 8075.
(16) Ohkita, M.; Ando, K.; Tsuji, T. *Chem. Commun.* **2001**, 2570.
(17) Srinivasan, M.; Sankararaman, S.; Hopf, H.; Varghese, B. *Eur. J. Org. Chem.* **2003**, 660.
(18) Hosokawa, Y.; Kawase, T.; Oda, M. *Chem. Commun.* **2001**, 1948.
(19) Aviram, A.; Ratner, M. A. *Chem. Phys. Lett.* **1974**, *29*, 277.
(20) (a) Metzger, R. M. *Synth. Met.* **2001**, *124*, 107. (b) Fischer, C. M.; Burghard, M.; Roth, S. *Synth. Met.* **1995**, *71*, 1975.
(21) Luo, Y.; Collier, C. P.; Jeppesen, J. O.; Nielsen, K. A.; DeIonno, E.; Ho, G.; Perkins, J.; Tseng, H. R.; Yamamoto, T.; Stoddart, J. F.; Heath, J. R. *ChemPhysChem* **2002**, *3*, 519.
(22) Pease, A. R.; Jeppesen, J. O.; Stoddart, J. F.; Luo, Y.; Collier, C. P.; Heath, J. R. *Acc. Chem. Res.* **2001**, *34*, 433.
(23) Yang, Z. Q.; Lang, N. D.; Di Ventra, M. *Appl. Phys. Lett.* **2003**, *82*, 1938.
(24) Ali, M. A.; Krishnan, M. S. *Mol. Phys.* **2009**, *107*, 2149.
(25) Segawa, Y.; Omachi, H.; Itami, K. *Org. Lett.* **2010**, *12*, 2262.
(26) von Baeyer, A. *Ber. Dtsch. Chem. Ges.* **1885**, *18*, 2278.
(27) Westheimer, F. H. *The Chemical Society, London*; Special Publication No. 8; Royal Society of Chemistry: London, 1957; p 1.
(28) Dudev, T.; Lim, C. *J. Am. Chem. Soc.* **1998**, *120*, 4450.
(29) Hehre, W. J.; Ditchfield, R.; Radom, L.; Pople, J. A. *J. Am. Chem. Soc.* **1970**, *92*, 4796.
(30) George, P.; Trachtman, M.; Bock, C. W.; Brett, A. M. *Tetrahedron* **1976**, *32*, 317.
(31) Wheeler, S. E.; Houk, K. N.; Schleyer, P. R.; Allen, W. D. *J. Am. Chem. Soc.* **2009**, *131*, 2547.

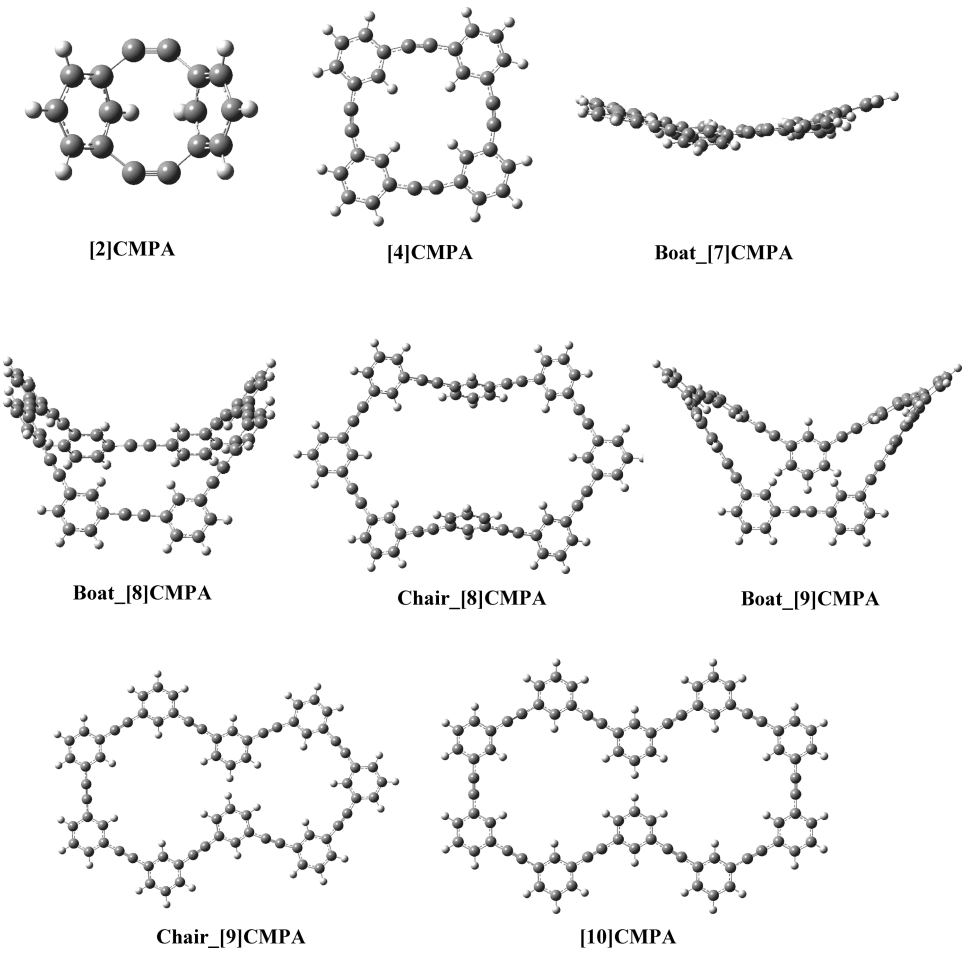

FIGURE 2. Optimized geometries of a few [*n*]CMPAs at the B3LYP/6-31G* level of theory.

used homodesmotic reactions in combination with density functional theory for calculating the strain energies in this paper because of the likely cancellation of errors in computation due to chemically similar reactants and products. Pople and co-workers introduced the isodesmic reaction concept for the first time, to our knowledge, for calculations of the thermodynamic properties.[29] Since then, other types of chemical reactions have been used that improve on the isodesmic reaction method. Homodesmotic reactions are widely used for calculation of the thermodynamic properties of bigger cyclic and noncyclic systems.[24,25,30,31] It is difficult to carry out experimental studies on a majority of these macrocycles in the gas phase. Theoretical methods are currently the only means for providing meaningful data on some of these macrocycles. The chemical and electronic properties of [*n*]CMPAs and [*n*]CPPAs are quite dependent on the ring sizes of the macrocycles. Theoretical calculations of new macrocyclic structures, B-B[4_n]MCs and B-B[4_n]PCs, known as "big brother"[11,12] of [*n*]CMPAs and [*n*]CPPAs have also been reported in this paper. Li et al. have reported the strain energies and electronic properties of [*n*]CMPAs using the HF/6-31G* level of theory.[32] We have improved this as well as extended the approach to include the strain energies of [*n*]CMPAs, B-B[4_n]MCs, and B-B[4_n]PCs using homodesmotic reactions coupled with B3LYP/6-31G*, mPW1PW91/6-31G*, and M06-2X/6-31+G**//B3LYP/6-31G* levels of theory. The standard enthalpy of formation, electronic properties, and spectroscopic constants for these oligomers ([*n*]CMPAs, B-B[4_n]MCs, and B-B[4_n]PCs) are also provided at the same levels of theory, which will be helpful in understanding their packing model in solids and in designing and rationalizing the molecular architecture for molecular electronics.

2. Computational Method

The structures of [*n*]CMPAs, B-B[4_n]MCs, B-B[4_n]PCs, 1,3-diethynylbenzene, 1,3-di(buta-1,3-diynyl)benzene [*m*-bis(butadiynyl)benzene], 1,4-di(buta-1,3-diynyl)benzene [*p*-bis(butadiynyl)-benzene], and acetylenes were optimized at the B3LYP/6-31G* and mPW1PW91/6-31G* levels of theory.[33−35] The polymeric structures of [*n*]CMPAs, B-B[4_n]MCs, and B-B[4_n]PCs are given in parts a−c of Figure 1, respectively. The optimized geometries of some of these oligomers calculated using the B3LYP/6-31G* level of theory are given in Figures 2−4. The optimized geometries were also verified to be the real minima from vibrational analysis by the same level of theory and the basis set that showed no imaginary frequency. The Cartesian coordinates and vibrational frequencies of [*n*]CMPAs, B-B[4_n]MCs, B-B[4_n]PCs, 1,3-diethynylbenzene, 1,3-di(buta-1,3-diynyl) benzene, and 1,4-di(buta-1,3-diynyl)benzene are given in the Supporting Information for

(32) Li, Y.; Zhao, J.; Yin, X.; Yin, G. *ChemPhysChem* **2006**, *7*, 2593.

(33) Becke, A. D. *J. Chem. Phys.* **1993**, *98*, 5648.
(34) Francl, M. M.; Pietro, W. J.; Hehre, W. J.; Binkley, J. S.; Gordon, M. S.; Defrees, D. J.; Pople, J. A. *J. Chem. Phys.* **1982**, *77*, 3654.
(35) Adamo, C.; Barone, V. *J. Chem. Phys.* **1998**, *108*, 664.

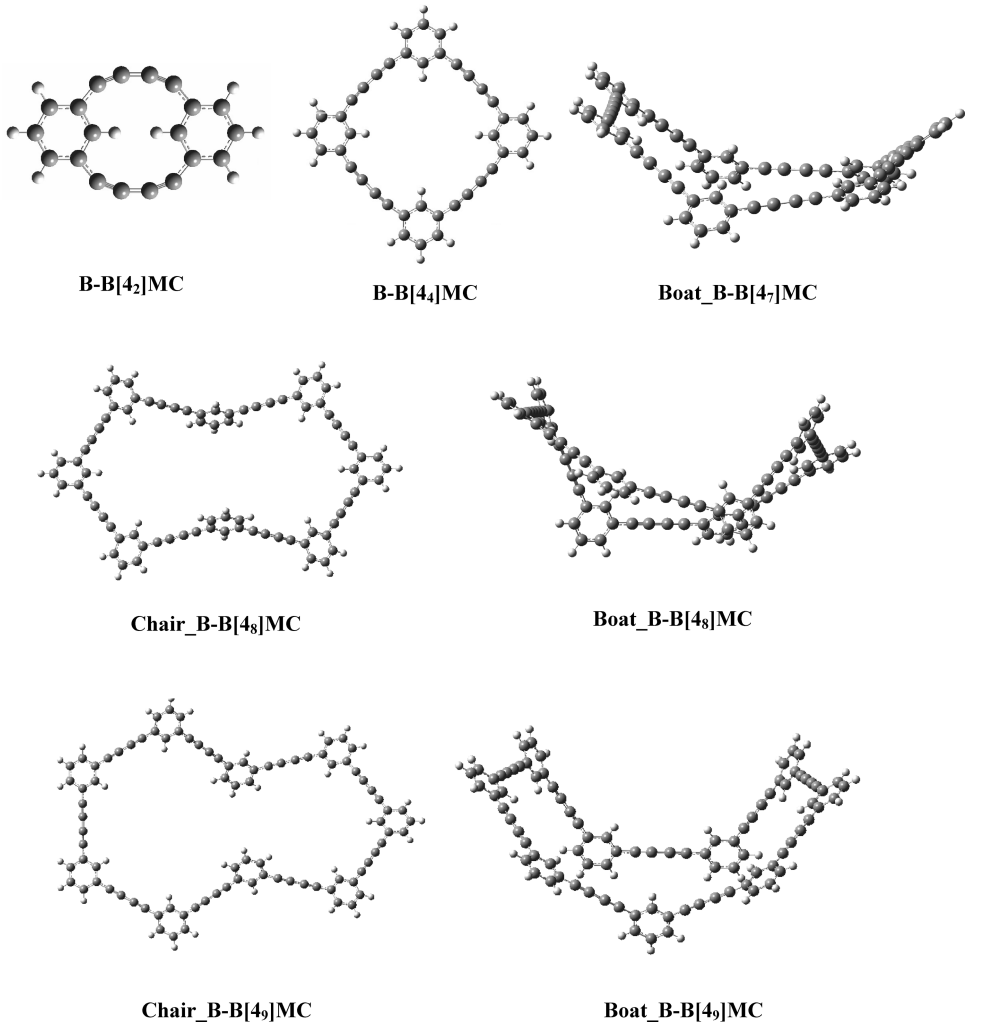

FIGURE 3. Optimized geometries of a few B-B[4$_n$]MCs at the B3LYP/6-31G* level of theory.

the benefit of the reader. We have also used the functional mPW1PW91 in combination with the 6-31G* basis set for cyclic phenyleneacetylenes (CPAs) and found that the results are very close to those based on B3LYP. For the report given here, we have restricted ourselves to the use of the B3LYP/mPW1PW91/6-31G* level of theory for all electronic structure calculations. We have also done single-point energy calculation using the M06-2X functional[36] with the 6-31+G** basis set using the optimized geometry from the B3LYP/6-31G* level of theory. Polarized and diffused basis sets like 6-31G**, 6-31+G*, 6-31+G**, and 6-311++G** are computationally more expensive for vibrational frequency analysis but do not alter significantly the results, as verified by their use by us for smaller [*n*]CMPAs, B-B[4$_n$]MCs, and B-B[4$_n$]PCs. Therefore, the basis set 6-31G* was chosen for all members of [*n*]CMPAs, B-B[4$_n$]MCs, and B-B[4$_n$]PCs. In addition, we have also calculated proton nuclear magnetic resonance (^{1}H NMR) chemical shifts using the gauge-independent atomic orbital (GIAO) method.[37] Electronic structure calculations were carried out with *Gaussian 03* and *Gaussian 09* suites of programs.[38,39]

3. Results and Discussion

3.A. Strain Energies and Heats of Formation of [*n*]CMPAs and B-B[4$_n$]MCs. 3.A.I. Strain Energies. In order to understand the pattern of strain energies with respect to *n*, the bond lengths and angles of [2]CMPA−[6]CMPA are provided in the Supporting Information. Here, they are reproduced for [3]CMPA and [4]CMPA, with atom labels (Figure 5) and numerical values in Table 1. Table 1 also contains a comparison between the theoretical values and experimental data.[5]

(36) Zhao, Y.; Truhlar, D. G. *Theor. Chem. Acc.* **2008**, *120*, 215.

(37) (a) London, F. *J. Phys. Radium* (*Paris*) **1937**, *94*, 4959. (b) McWeeny, R. *Phys. Rev.* **1962**, *126*, 1028. (c) Ditchfield, R. *Mol. Phys.* **1974**, *27*, 789. (d) Dodds, J. L.; McWeeny, R.; Sadlej, A. J. *Mol. Phys.* **1980**, *41*, 1419. (e) Wolinski, K.; Hilton, J. F.; Pulay, P. *J. Am. Chem. Soc.* **1990**, *112*, 8251.

(38) Frisch, M. J.; Trucks, G. W.; Schlegel, H. B.; Scuseria, G. E.; Robb, M. A.; Cheeseman, J. R.; Montgomery, J. A., Jr.; Vreven, T.; Kudin, K. N.; Burant, J. C.; Millam, J. M.; Iyengar, S. S.; Tomasi, J.; Barone, V.; Mennucci, B.; Cossi, M.; Scalmani, G.; Rega, N.; Petersson, G. A.; Nakatsuji, H.; Hada, M.; Ehara, M.; Toyota, K.; Fukuda, R.; Hasegawa, J.; Ishida, M.; Nakajima, T.; Honda, Y.; Kitao, O.; Nakai, H.; Klene, M.; Li, X.; Knox, J. E.; Hratchian, H. P.; Cross, J. B.; Bakken, V.; Adamo, C.; Jaramillo, J.; Gomperts, R.; Stratmann, R. E.; Yazyev, O.; Austin, A. J.; Cammi, R.; Pomelli, C.; Ochterski, J. W.; Ayala, P. Y.; Morokuma, K.; Voth, G. A.; Salvador, P.; Dannenberg, J. J.; Zakrzewski, V. G.; Dapprich, S.; Daniels, A. D.; Strain, M. C.; Farkas, O.; Malick, D. K.; Rabuck, A. D.; Raghavachari, K.; Foresman, J. B.; Ortiz, J. V.; Cui, Q.; Baboul, A. G.; Clifford, S.; Cioslowski, J.; Stefanov, B. B.; Liu, G.; Liashenko, A.; Piskorz, P.; Komaromi, I.; Martin, R. L.; Fox, D. J.; Keith, T.; Al-Laham, M. A.; Peng, C. Y.; Nanayakkara, A.; Challacombe, M.; Gill, P. M. W.; Johnson, B.; Chen, W.; Wong, M. W.; Gonzalez, C.; Pople, J. A. *Gaussian 03*, revision E.01; Gaussian, Inc.: Wallingford, CT, 2004.

(39) Frisch, M. J. et al. *Gaussian 09*, revision A.1; Gaussian, Inc.: Wallingford, CT, 2009 (see the Supporting Information for the full reference).

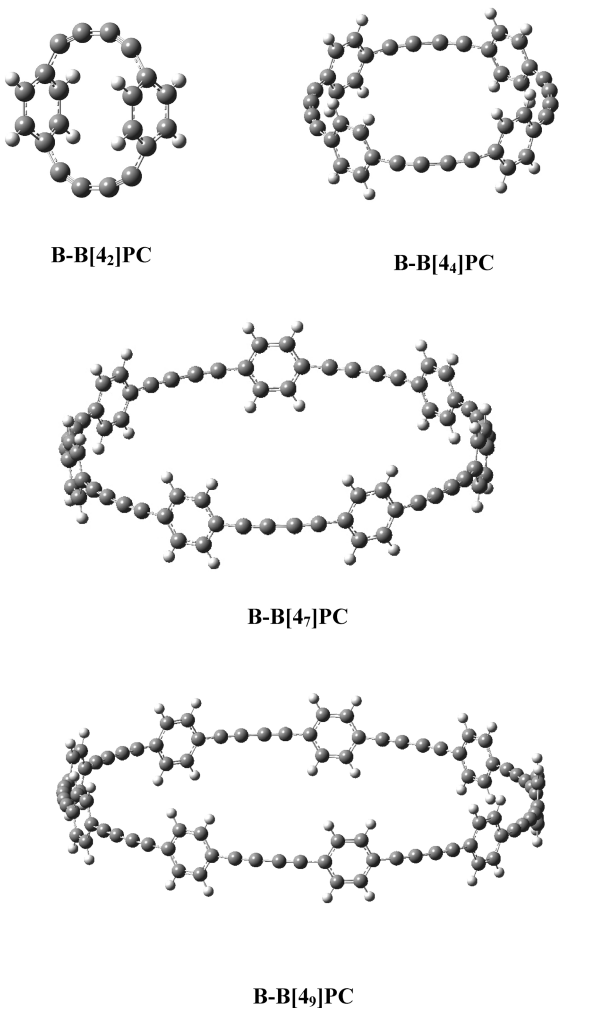

FIGURE 4. Optimized geometries of a few B-B[4_n]PCs at the B3LYP/6-31G* level of theory.

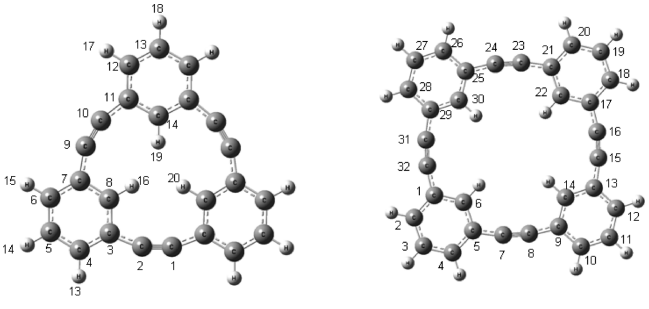

FIGURE 5. Optimized geometries of [3]CMPA and [4]CMPA with atom numbering obtained at the B3LYP/6-31G* level of theory.

The latter is available only for these macrocycles. These values are found to be in good agreement with each other.

The bent angles of [2]CMPA, [3]CMPA, [4]CMPA, [5]CMPA, and [6]CMPA ($sp^2-sp-sp$) were found to be 139.5°, 158.4°, 169.2°, 175.7°, and 179.9°, respectively. Homodesmotic reaction Scheme 1 was written in such a way that on the product side [6]CMPA is chosen as the reference system and is strain-free in the series of [*n*]CMPAs. [2]CMPA has the maximum strain in the [*n*]CMPA series and has not been synthesized so far. Strain energies for [3]CMPA, [4]CMPA, [5]CMPA, [6]CMPA, and [7]CMPA are less when compared to their para counterparts. Smaller values of the strain energies agree with the fact that [3]CMPA, [4]CMPA, [5]-CMPA, [6]CMPA, and [7]CMPA have been synthesized already.[5] Theoretical estimates of the strain energies of [*n*]CMPAs given by Li et al.[32] using the HF/6-31G* level of theory are compared with our values in Table 2. Kawase et al. have reported the strain energy of [4]CMPA to be 46.0 kJ mol^{-1} using molecular mechanics.[5c] We have computed strain energies using three different functionals, namely, B3LYP/6-31G*, mPW1PW91/6-31G*, and M06-2X/6-31+G**//B3LYP/6-31G* (Table 2). The strain energies of [*n*]CMPAs computed using B3LYP/6-31G* and mPW1P-W91/6-31G* levels of theory are very close to each other. In the case of the M06-2X/6-31+G**//B3LYP/6-31G* level of theory, the strain energy was observed to be different from the results of the B3LYP and mPW1PW91 functionals. This is possibly due to the fact that optimization was first done by using B3LYP/6-31+G* and single-point energy calculations were carried out using the M06-2X functional with the 6-31+G** basis set. Computational resources available to us do not permit us to explore this at the present time. In the case of [7]CMPA, [8]CMPA, [9]CMPA, and [10]CMPA, different conformers were observed. Boatlike conformations of [7]CMPA were observed to be the most stable. The torsional angle of [7]CMPA (177°) is less than that of the strain-free reference system [6]CMPA (180°). In the case of [8]CMPA and [9]CMPA, two stable conformers (boat and chairlike conformations) were observed. The energy difference between these two for [8]CMPA is found to be 5.5 kJ mol^{-1}, with the boat conformation being more stable than the chair conformation. The slight difference can be attributed to the rings in the chair form closing in slightly more than those in the boat form and causing nonbonding interactions (these are weak). The higher strain of [8]CMPA in both the chair and boatlike forms may be attributed to this. In the case of [9]CMPA, the opposite trend was observed; i.e., the energy difference between the boat and chair forms is 4.8 kJ mol^{-1}, with the boat conformer having a higher energy than the chair. In the case of [10]CMPA, only one stable form was observed and is shown in Figure 2. The structures are analogous to five- and six-membered rings, and the slightly enhanced stability is correlated to the shapes of these rings. The strain energies calculated for higher [*n*]CMPAs are thus reflections of their ring shapes. Our calculation of the strain energies of [*n*]CMPAs improved over previously obtained values with the inclusion of scaled zero-point energy, and the values are reported in Table 2. We have restricted our discussion only to stable forms of [*n*]CMPAs and note that planar forms of the rings of higher [*n*]CMPAs ([7]CMPA, [8]CMPA, [9]CMPA, and [10]CMPA) are of considerably higher energy as revealed by vibrational analysis.

Homodesmotic reaction schemes for B-B[4_n]MCs used in our calculations are similar to that of Scheme 1, with the product containing diacetylenic links between phenyl groups, namely, B-B[4_6]MC. The bending angles ($sp^2-sp-sp$ and $sp-sp-sp$) were calculated and found to be 150.5° and 158.8° (B-B[4_2]MC), 163.5° and 171.3° (B-B[4_3]MC), 170.8° and 176.5° (B-B[4_4]MC), 175.5° and 179.3° (B-B[4_5]MC), and 179.9° and 179.9° (B-B[4_6]MC) at the B3LYP/6-31G* level of theory. We have observed that the strain energies of

TABLE 1. Bond Lengths (Å) and Bond Angles (deg) of [3]CMPA and [4]CMPA at the B3LYP/6-31G* Level of Theory Compared with Experimental Values

[3]CMPA			[4]CMPA		
bond length/angle	B3LYP/6-31G*	expt	bond length/angle	B3LYP/6-31G*	expt
C1−C2[a]	1.220	1.193	C5−C7[a]	1.428	1.436
C9−C10	1.220	1.190	C7−C8	1.217	1.189
H16−H19	2.100	2.280	C8−C9	1.428	1.441
H16−H20	2.100	2.310	C13−C15	1.428	1.434
C1−C2−C3[b]	158.5	158.6	C15−C16	1.217	1.189
C2−C3−C4	128.9	129.0	C16−C17	1.428	1.445
C2−C3−C8	113.1	113.3	C21−C23	1.428	1.443
C4−C3−C8	117.9	117.6	C23−C24	1.217	1.195
C3−C4−C5	119.3	119.4	C24−C25	1.428	1.44
C4−C5−C6	122.1	122.4	C29−C31	1.428	1.447
C5−C6−C7	119.3	119.2	C31−C32	1.217	1.189
C3−C8−C7	123.2	123.3	C32−C1	1.428	1.438
C6−C7−C8	117.9	117.9	C5−C7−C8[b]	169.2	169.5
C8−C7−C9	113.1	112.9	C7−C8−C9	169.2	169.9
C7−C9−C10	158.5	158.7	C13−C15−C16	169.2	168.2
C9−C10−C11	158.5	158.4	C15−C16−C17	169.2	167.7
C10−C11−C12	128.9	129.2	C21−C23−C24	169.2	169.4
C11−C12−C13	119.3	119.8	C23−C24−C25	169.2	169
C10−C11−C14	113.1	113.2	C29−C31−C32	169.2	168.6
			C31−C32−C1	169.2	167.7

[a]Bond length (Å). [b]Bond angle (deg).

SCHEME 1. Homodesmotic Reaction Scheme Containing Cyclic [6]CMPA as a Reference Molecule[a]

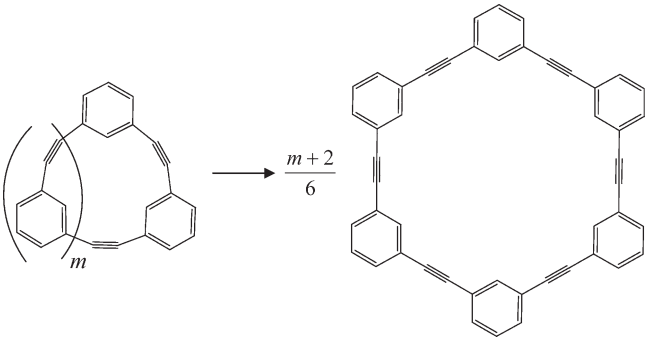

[a]In this scheme, *m* represents the number of phenylacetylene groups. When $m = 1$, the strain energy of [3]CMPA will be given.

B-B[4_n]MCs are lower than the corresponding [*n*]CMPAs because the bent angle is closer to 180° compared to that of [*n*]CMPAs. Higher members of B-B[4_n]MCs such as B-B[4_7]MC, B-B[4_8]MC, and B-B[4_9]MC are observed to be in the same conformational states as their [*n*]CMPAs counterparts. The boat conformation of B-B[4_8]MC is more stable than the chair form by 1.7 kJ mol^{-1}, which is also reflected by a lower strain energy for this conformer (Table 2). Zhao et al. have reported a difference of 1.3 kJ mol^{-1} energy between the chair and boat forms of B-B[4_8]MC.[40] In the case of B-B[4_9]MC, the chair conformation is more stable than the boat conformation by 1.6 kJ mol^{-1}. The strain energies per unit monomer are given in Figure 6 for various [*n*]CMPAs and B-B[4_n]MCs. This figure shows that the strain energy rapidly decreases to zero until $n = 6$ and increases for $n = 7$ and 8 but decreases subsequently in the case of $n = 9$, 10, etc.

We have also calculated strain energies of other metacyclophynes to find the effect of acetylenic groups in macrocycles. The strain energies per unit monomer of [$(2n+2)_2$]MCs and [$(2n+2)_3$]MCs, where $n = 2$ and 3, are shown in Figure 7 at the B3LYP/6-31G* level of theory. This figure indicates that the strain energy per unit monomer of metacyclophynes decreases as the number of acetylenic groups increases. The stability of these macrocycles is a function of the number of acetylenic groups in the oligomers. The structures of these metacyclophynes and a strain energy plot using mPW1PW91/6-31G* theory are given in the Supporting Information.

Specifically, our calculated values for some of these compounds are 151.5 kJ mol^{-1} ([6_2]MC), 111.3 kJ mol^{-1} ([8_2]MC), 59.8 kJ mol^{-1} ([6_3]MC), and 33.1 kJ mol^{-1} ([8_3]MC).

3.A.II. Heats of Formation. Because of the lack of reliable experimental heats of formation for these macrocycles, it is necessary to assess them by theoretical methods. The homodesmotic reaction Scheme 2a, coupled with the density functional theory method, is well suited also for calculation of the heats of formation of [*n*]CMPAs and is more accurate than other schemes because of chemically similar species on both sides. However, experimental heats of formation of 1,3-diethynylbenzene are unknown. Therefore, our estimates are dependent only upon the theoretical values and can be used to observe trends in ΔH's between different *n*-mers. Theoretical heats of formation of 1,3-diethynylbenzene were calculated using another homodesmotic reaction (Scheme 2b).

Hence, our scheme for calculation of the heats of reaction is equivalent to the sum of reactions in Scheme 2. Experimental gas-phase heats of formation[41,42] of benzene (82.8 kJ mol^{-1}), propene (20.4 kJ mol^{-1}), and 2-methyl-1-buten-3-yne (258.6 kJ mol^{-1}) were used to obtain values of 561.7 and 562.6 kJ mol^{-1} at the B3LYP/6-31G* and mPW1PW91/6-31G* levels of theory. The heat of formation of 1,3-diethynylbenzene has

(40) Zhao, J.; Li, Y.; Liu, H.; Li, P.; Yin, G. *THEOCHEM* **2008**, *861*, 7.

(41) NIST Computational Chemistry Comparison and Benchmark Database. National Institute of Standards and Technology: Gaithersburg, MD, 20899; http://srdata.nist.gov/cccbdb/, release Oct 9, 2003.

(42) Afeefy, H. Y.; Liebman, J. F.; Stein, S. E. Neutral Thermochemical Data in NIST Chemistry WebBook, Standard Reference Database Number 69. Linstrrom, P. J, Mallard, W. G., Eds.; National Institute of Standard and Technology: Gaithersburg, MD, 20899; http://webbook.nist.gov, March 2003.

TABLE 2. Strain Energies (kJ mol^{-1}) of [*n*]CMPAs Using Homodesmotic Reaction Scheme *1* and Its Analogue for B-B[4_n]MCs at the B3LYP/6-31G*, mPW1PW91/6-31G*, and M06-2X/6-31+G Levels of Theory**

[*n*]CMPAs	B3LYP/6-31G*	mPW1PW91/6-31G*	M06-2X/6-31+G**[a]	HF/6-31G*[b]	B-B[4_n]MCs	B3LYP/6-31G*	mPW1PW91/6-31G*	M06-2X/6-31+G**[a]
[2]CMPA	445.9	443.6	435.5		B-B[4_2]MC	229.0	229.3	227.9
[3]CMPA	153.8	153.7	147.2	159.7, 190.6	B-B[4_3]MC	83.6	82.1	84.8
[4]CMPA	48.9	48.4	47.4	54.2, 59.4 (46.0)[c]	B-B[4_4]MC	30.9	29.2	28.6
[5]CMPA	9.7	9.4	9.9	10.3, 11.5	B-B[4_5]MC	8.2	5.8	6.2
[6]CMPA	0.0	0.0	0.0	0.0, 0.0	B-B[4_6]MC	0.0	0.0	0.0
[7]CMPA[d]	6.9	6.6	6.6	4.2, 4.5	B-B[4_7]MC[d]	2.9	2.7	0.7
[8]CMPA[e]	17.6	16.6	13.2	8.8, 8.2	B-B[4_8]MC[e]	5.3	4.9	1.8
[8]CMPA[d]	12.1	11.6	9.7	5.8, 5.4	B-B[4_8]MC[d]	3.5	3.3	1.3
[9]CMPA[e]	7.5	6.4	5.3	10.2, 9.8	B-B[4_9]MC[e]	2.2[f]	3.2	0.7
[9]CMPA[d]	12.1	11.4	9.9	7.6, 7.3	B-B[4_9]MC[d]	3.2[f]	4.8	1.7

[a]Single-point energy calculation at the M06-2X/6-31+G**//B3LYP/6-31G* level. [b]Calculated by Li et al. [c]Calculated by Kawase et al. [d]Boat form. [e]Chair form. [f]Without zero-point energy.

been also calculated using quantum chemistry composite methods such as G3MP2, G3B3, and G3MP2B3 theories,[43,44] and these values are 560.9, 561.4, and 562.7 kJ mol^{-1}, respectively. We have observed that heats of formation using density functional theories (B3LYP and mPW1PW91) are consistent with ab initio quantum chemistry (G3MP2, G3B3, and G3MP2B3) methods (Table 3).

Heats of formation $\Delta H^0_{f,298K}$ of [*n*]CMPAs can be calculated using the following identity:

$$\Delta H^0_f([n]\text{CMPAs}) = -\Delta H^0_{rxn} + (m+2)\Delta H^0_f(1,3\text{-diethynylbenzene}) - (m+2)\Delta H^0_f(C_2H_2) \quad (1)$$

$\Delta H^0_{f,298K}/n$ of [*n*]CMPAs decreases until *n* becomes 6, then increases with *n*, and finally decreases as *n* becomes larger than 8. $\Delta H^0_{f,298K}$ and $\Delta H^0_{f,298K}/n$ of [*n*]CMPAs (per unit monomer) are given for various values of *n* in Table 4. The $\Delta H^0_{f,298K}/n$ value of [*n*]CMPAs per unit monomer also correlates well with the molecular strain.

Heats of formation of B-B[4_n]MCs were calculated using the homodesmotic reaction Scheme 3.

Experimental gas-phase $\Delta H^0_{f,298K}$ values of acetylene (226.7 kJ mol^{-1}) and 1,3-butadiyne (464.4 kJ mol^{-1}) were used for calculation of the heats of formation of 1,3-di(buta-1,3-diynyl)benzene (*m*-$C_{14}H_6$). $\Delta H^0_{f,298K}$ of 1,3-di(buta-1,3-diynyl)benzene was found to be 1029.1 and 1029.4 kJ mol^{-1} at the B3LYP/6-31G* and mPW1PW91/6-31G* levels of theory, respectively. The heats of formation of *m*-$C_{14}H_6$ using G3MP2 (1027.7 kJ mol^{-1}), G3B3 (1024.6 kJ mol^{-1}), and G3MP2B3 (1026.5 kJ mol^{-1}) theories are close to those of the B3LYP/6-31G* (1029.1 kJ mol^{-1}) and mPW1PW91/6-31G* ((1029.4 kJ mol^{-1}) levels of theory.

$\Delta H^0_{f,298K}$ and $\Delta H^0_{f,298K}/n$ of B-B[4_n]MCs are given in Table 4. Tobe et al.[15] have calculated $\Delta H^0_{f,298K}/n$ for B-B[4_4]MC (541.5 kJ mol^{-1}) and B-B[4_6]MC (531.9 kJ mol^{-1}) using a semiempirical (AM1) method. We have obtained different values of $\Delta H^0_{f,298K}/n$ for B-B[4_4]MC (571.2 kJ mol^{-1}) and B-B[4_6]MC (564.2 kJ mol^{-1}) improved over this method. We believe that our values are more accurate because of the appearance of systematic trends in $\Delta H^0_{f,298K}/n$ for various *n* values. $\Delta H^0_{f,298K}$ values of B-B[4_n]MCs were calculated using B3LYP/6-31G* and mPW1PW91/6-31G* and were found to be less compared to those of B-B[4_n]PCs (Table 5), which might be attributed to the higher values of bend angles in the case of B-B[4_n]MCs. $\Delta H^0_{f,298K}/n$ values for different *n*'s are given in Table 4. The heat of formation per unit monomer of 1-(buta-1,3-diynyl)benzene also correlates well with the strain energies of B-B[4_n]MCs, as shown in Figure 8.

3.B. Strain Energies and Heats of Formation in B-B[4_n]-PCs. 3.B.I. Strain Energies. The geometries of B-B[4_n]PCs optimized at the B3LYP/6-31G* level of theory are given in Figure 4. In the case of B-B[4_n]PCs, maximum strain energies arise mainly because of deviation of the acetylene moieties from linearity. The calculated bending angles ($sp^2-sp-sp$ and $sp-sp-sp$) are given in brackets following the compound, namely, B-B[4_2]PC (143.3° and 159.0°), B-B[4_3]PC (157.7° and 163.9°), B-B[4_4]PC (162.7° and 168.6°), B-B[4_5]PC (167.3° and 169.3°), B-B[4_6]PC (168.5° and 172.7°), B-B[4_7]PC (170.1° and 173.7°), B-B[4_8]PC (171.3° and 174.6°), and B-B[4_9]PC (172.4° and 175.3°). Ohkita et al. earlier calculated the bend angles for B-B[4_6]PC (170.8° and 171.2°) using the semiempirical (PM3) method.[16] These angles are closer to the strain-free values than those reported here. However, the bend angles of B-B[4_n]PCs are found to be less than the corresponding ones for [*n*]CPPAs because of the extended diameter of the ensuing ring in the case of two acetylenic groups connecting the phenyl groups. The strain energies (in kJ mol^{-1}) of B-B[4_n]PCs were calculated using homodesmotic reaction Scheme 4 coupled with density functional theory (B3LYP/6-31G*, mPW1PW91/6-31G*, and M06-2X/6-31+G**) and are given in Table 5.

Srinivasan et al. have calculated the strain energies of B-B[4_2]PC and B-B[4_3]PC using semiempirical (AM1 and PM3) methods.[17] These values are given in Table 5. The strain energies calculated by them using the AM1 method are underestimated compared with our results, but the results of the PM3 method are close to our results. The strain energies per unit monomer of B-B[4_n]PCs and [*n*]CPPAs are given in Figure 9, and it can be seen that the strain energies per unit monomer approach a constant value as the number of 1-(buta-1,3-diynyl)benzene units increases and are less than those for [*n*]CPPAs. Recently, Itami et al. computed the strain energies of [*n*]cycloparaphenylenes ([*n*]CPPs) using homodesmotic reaction methods at the B3LYP/6-31G* level of theory.[25] They have reported that the strain energies of [*n*]CPPs

(43) Curtiss, L. A.; Redfern, P. C.; Raghavachari, K.; Rassolov, V.; Pople, J. A. *J. Chem. Phys.* **1999**, *110*, 4703.
(44) Baboul, A. G.; Curtiss, L. A.; Redfern, P. C.; Raghavachari, K. *J. Chem. Phys.* **1999**, *110*, 7650.

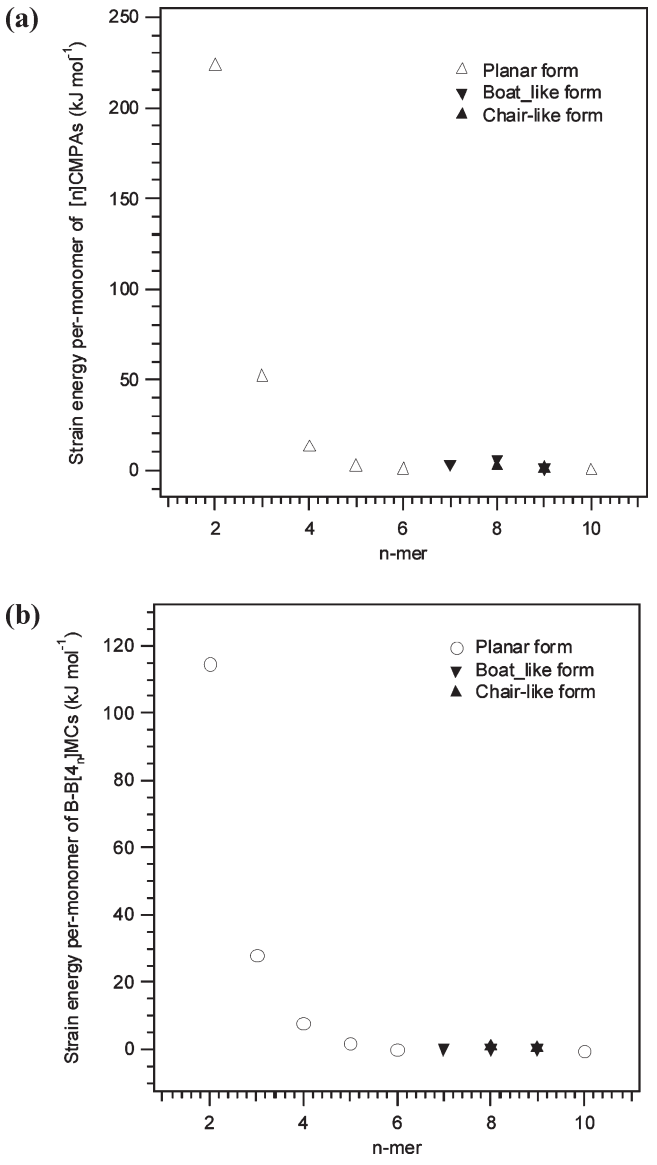

FIGURE 6. Strain energy per unit monomer of [*n*]CMPAs and B-B[4_n]MCs calculated at the B3LYP/6-31G* level of theory.

are higher than those of [*n*]CPPAs. We have also compared the strain energies of ring types of oligomers such as [*n*]CPPs, [*n*]CPPAs, and B-B[4_n]PCs using B3LYP/6-31G*, mPW1PW91/6-31G*, and M06-2X/6-31+G** levels of theory and found that the order for the strain energies is [*n*]CPPs > [*n*]CPPAs > B-B[4_n]PCs.

We have carried out calculations on [$(2n+2)_2$]PCs and [$(2n+2)_3$]PCs (n = 2 and 3). The strain energies of [6_2]PC (297.9 kJ mol^{-1}), [6_3]PC (214.2 kJ mol^{-1}), [8_2]PC (228.9 kJ mol^{-1}), and [8_3]PC (140.6 kJ mol^{-1}), obtained using the B3LYP/6-31G* level of theory, lead us to the same conclusion as that in the case of [m_n]MCs, where the strain energy decreases as the number of acetylenic groups increases. The strain energies per unit monomer of [$(2n+2)_2$]PCs and [$(2n+2)_3$]PCs at the B3LYP/6-31G* level of theory are given in Figure 7. This suggests that highly reactive [m_n]PCs with longer $C_{sp}-C_{sp}$ bonds may become useful precursors of small carbon clusters with a specific carbon number. The structures of these paracyclophynes are given in the Supporting Information.

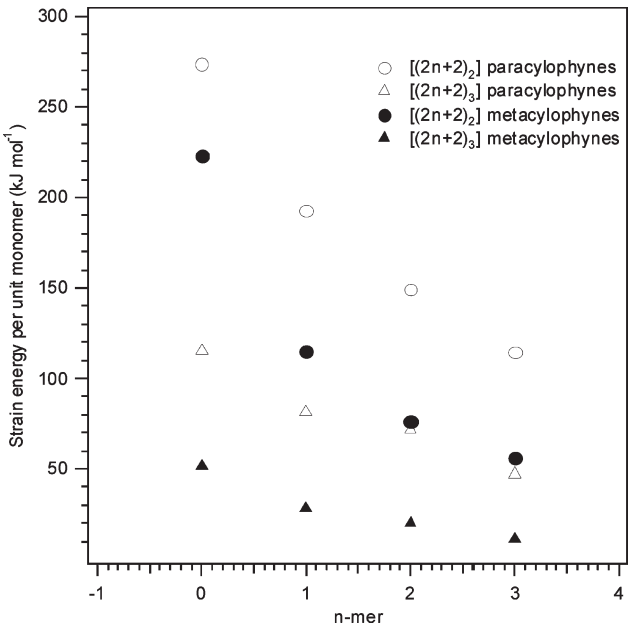

FIGURE 7. Strain energy per unit monomer of [$(2n+2)_2$]MCs, [$(2n+2)_3$]MCs, [$(2n+2)_2$]PCs, and [$(2n+2)_3$]PCs calculated at the B3LYP/6-31G* level of theory.

SCHEME 2. Homodesmotic Reaction Schemes for Calculation of the Heats of Formation of (a) [*n*]CMPAs and (b) 1,3-Diethynylbenzene

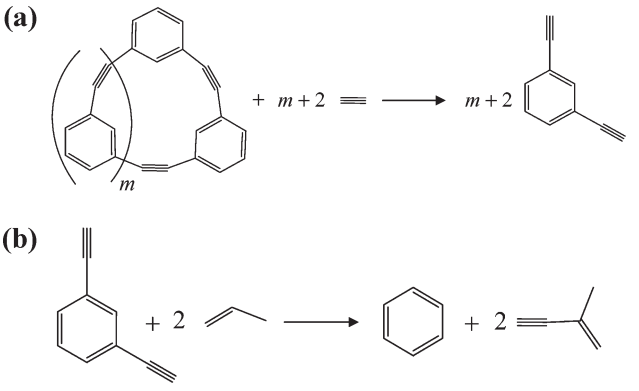

3.B.II. Heats of Formation. The heats of formation of B-B[4_n]PCs were calculated using the homodesmotic reaction Scheme 5a,b.

Experimental gas-phase[41,42] $\Delta H^0_{f,298K}$ for acetylene and 1,3-butadiyne and the theoretically calculated value[24] for 1,4-diethynylbenzene (559.5 kJ mol^{-1}) have been used for calculation of the heats of formation of 1,4-di(buta-1,3-diynyl)-benzene (p-$C_{14}H_6$). $\Delta H^0_{f,298K}$ of 1,4-di(buta-1,3-diynyl)benzene has been found to be 1025.5 kJ mol^{-1}. The heats of formation of 1,4-di(buta-1,3-diynyl)benzene (p-$C_{14}H_6$) using mPW1PW91/6-31G*, G3MP2, G3B3, and G3MP2B3 are given in Table 3.

$\Delta H^0_{f,298K}$ values of B-B[4_n]PCs and values for per unit monomer are given in Table 5. $\Delta H^0_{f,298K}$ values per unit monomer of B-B[4_n]PCs are given in Figure 8. These values also correlate well with the strain energies.

3.C. Spectroscopic Properties of [*n*]CMPAs, B-B[4_n]MCs, and B-B[4_n]PCs. Vibrational analysis has been carried out on

TABLE 3. Heats of Formation (kJ mol^{-1}) of Phenylacetylene, 1,4-Diethynylbenzene, 1,3-Diethynylbenzene, 1,4-Di(buta-1,3-diynyl)benzene, and 1,3-Di(buta-1,3-diynyl)benzene at Different Levels of Theory

	B3LYP/6-31G*	mPW1PW91/6-31G*	G3MP2	G3B3	G3MP2B3	expt[41]
C_8H_6[a]	321.1	321.6	321.8	321.0	320.8	306.6
p-$C_{10}H_6$	559.5	560.3	560.6	560.1	561.5	
m-$C_{10}H_6$	561.7	562.6	560.9	561.4	562.7	
p-$C_{14}H_6$	1025.5	1025.7	1026.0	1022.9	1024.9	
m-$C_{14}H_6$	1029.1	1029.4	1027.7	1024.6	1026.5	

[a]Phenylacetylene.

TABLE 4. Heats of Formation (kJ mol^{-1}) of [*n*]CMPAs and B-B[4$_n$]MCs at the B3LYP/6-31G* and mPW1PW91/6-31G* Levels of Theory

	B3LYP/6-31G*		mPW1PW91/6-31G*			B3LYP/6-31G*		mPW1PW91/6-31G*	
[*n*]CMPAs	$\Delta H^0_{f,298K}$	$\Delta H^0_{f,298K}/n$	$\Delta H^0_{f,298K}$	$\Delta H^0_{f,298K}/n$	B-B[4$_n$]MCs	$\Delta H^0_{f,298K}$	$\Delta H^0_{f,298K}/n$	$\Delta H^0_{f,298K}$	$\Delta H^0_{f,298K}/n$
[2]CMPA	1109.9	555.0	1109.1	554.6	B-B[4$_2$]MC	1355.1	677.6	1356.0	678.0
[3]CMPA	1158.8	386.3	1149.0	383.0	B-B[4$_3$]MC	1773.5	591.2	1773.3	591.1
[4]CMPA	1380.9	345.3	1382.7	345.7	B-B[4$_4$]MC	2284.8	571.2 (541.5)[a]	2285.0	571.2
[5]CMPA	1676.2	335.2	1678.7	335.8	B-B[4$_5$]MC	2827.5	565.5	2827.3	565.5
[6]CMPA	2001.0	333.5	2004.1	334.0	B-B[4$_6$]MC	3385.1	564.2 (531.9)[a]	3386.7	564.5
[7]CMPA[b]	2342.2	334.6	2345.7	335.1	B-B[4$_7$]MC[b]	3952.9	564.7	3950.1	564.3
[8]CMPA[c]	2687.4	335.9	2690.7	336.3	B-B[4$_8$]MC[c]	4520.4	565.1	4520.7	565.1
[8]CMPA[b]	2678.4	334.8	2685.5	335.7	B-B[4$_8$]MC[b]	4518.5	564.8	4520.0	565.0
[9]CMPA[c]	3010.9	334.6	3014.8	335.0	B-B[4$_9$]MC[c]				
[9]CMPA[b]	3014.1	334.9	3020.3	335.6	B-B[4$_9$]MC[b]				
[10]CMPA	3337.1	333.7	3342.0	334.2					

[a]Calculated by Tobe et al.[15] [b]Boat form. [c]Chair form.

TABLE 5. Strain Energy (kJ mol^{-1}) and Heats of Formation (kJ mol^{-1}) of B-B[4$_n$]PCs Using Homodesmotic Reaction Schemes 4 and 5

	strain energy			B3LYP/6-31G*		mPW1PW91/6-31G*	
B-B[4$_n$]PCs	B3LYP/6-31G*	mPW1PW91/6-31G*	M06-2X/6-31+G**[a]	$\Delta H^0_{f,298K}$	$\Delta H^0_{f,298K}/n$	$\Delta H^0_{f,298K}$	$\Delta H^0_{f,298K}/n$
B-B[4$_2$]PC	385.1 (443.5, 389.1)[b]	383.6	384.8	1512.3	756.2	1507.9	754.0
B-B[4$_3$]PC	243.2 (288.7, 251.0)[b]	242.9	252.8	1936.2	645.4	1930.2	643.4
B-B[4$_4$]PC	172.0	170.4	187.2	2429.7	607.4	2421.4	605.4
B-B[4$_5$]PC	124.2	129.4	146.2	2947.0	589.4	2940.0	588.0
B-B[4$_6$]PC	97.1	96.6	118.3	3484.4	580.7	3473.5	578.9
B-B[4$_7$]PC	73.7	73.5	96.9	4026.0	575.1	4013.6	573.4
B-B[4$_8$]PC	55.0	55.6	80.0	4572.2	571.5	4558.6	569.8
B-B[4$_9$]PC	39.8	40.0	66.1	5122.1	569.1	5106.6	567.4

[a]Single-point energy calculation at the M06-2X/6-31+G**//B3LYP/6-31G* level. [b]Calculated by Srinivasan et al.[17]

SCHEME 3. Homodesmotic Reaction Schemes for Calculation of the Heats of Formation of (a) B-B[4$_n$]MCs and (b) 1,3-Di(buta-1,3-diynyl)benzene

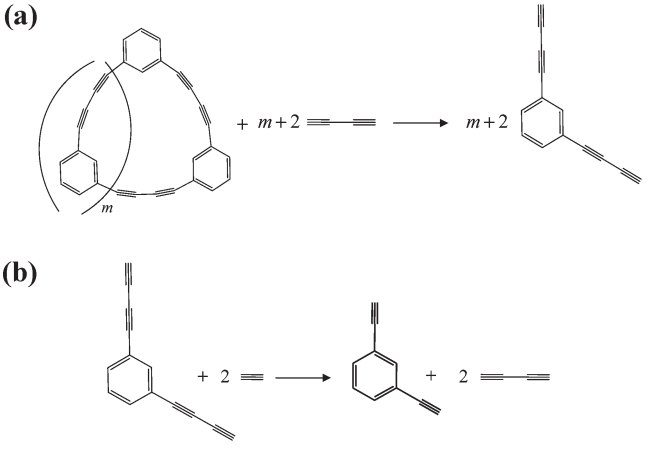

[*n*]CMPAs, B-B[4$_n$]MCs, and B-B[4$_n$]PCs at the B3LYP/6-31G* and mPW1PW91/6-31G* levels of theory, and all configurations are observed to be stable (no imaginary frequency). Raman frequencies of the −C≡C− stretches of [3]CMPA, [4]-CMPA, and [6]CMPA have been observed experimentally[5b,c]

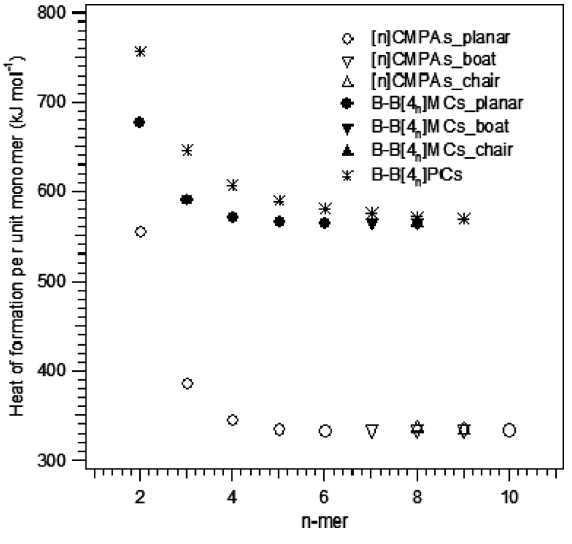

FIGURE 8. Heat of formation per unit monomer of [*n*]CMPAs, B-B[4$_n$]MCs, and B-B[4$_n$]PCs calculated using the B3LYP/6-31G* level of theory.

($\tilde{\nu}$ = 2155, 2202.5, and 2223 cm^{-1}) and are compared here with the theoretically calculated values, which are given in

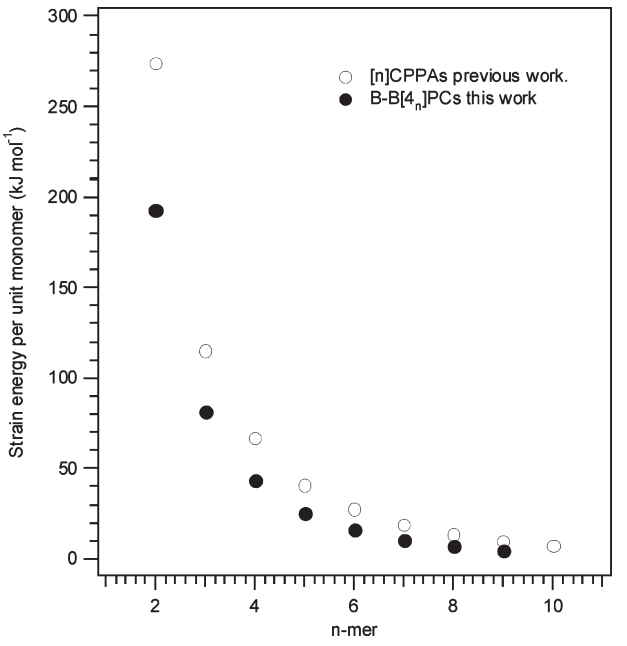

FIGURE 9. Strain energy per unit monomer of [*n*]CPPAs and B-B[4_n]PCs calculated at the B3LYP/6-31G* level of theory.

TABLE 6. Scaled Vibrational Frequencies (cm^{-1}) and ^{1}H NMR Chemical Shifts (ppm) of [*n*]CMPAs and B-B[4_n]MCs at the B3LYP/6-31G* Level of Theory

[*n*]CMPAs	−C≡C− frequencies	^{1}H NMR chemical shifts
[2]CMPA	2050	6.88 (4H), 7.10 (2H), 9.21 (2H)
[3]CMPA	2163 (2155)[a]	7.19 (6H) [7.23 (6H)] [a], 7.45 (3H) [7.35 (3H)] [a], 8.30 (3H) [8.38 (3H)][a]
[4]CMPA	2212 (2202)[a]	7.35 (8H), 7.42 (4H) [7.35 (12H)][a], 8.19 (4H) [8.07 (4H)][a]
[5]CMPA	2224	7.45 (15H), 7.96 (5H)
[6]CMPA	2226 (2223)[a]	7.50 (18H), 7.80 (6H)
[7]CMPA[b]	2225	7.46 (7H), 7.58 (14H), 7.69 (7H)
[8]CMPA[c]	2227, 2232	7.50 (24H), 7.67 (2H), 7.77(6H)
[8]CMPA[b]	2216, 2232	7.43 (8H), 7.53 (16H), 7.73 (8H)
[9]CMPA[c]	2225	8.02 (1H), 7.93 (2H), 7.82 (4H), 7.69 (6H), 7.64 (23H)
[9]CMPA[b]	2226, 2233	7.49 (27H), 7.71 (9H)
[10]CMPA	2226	7.71 (10H), 7.69 (4H), 7.57 (18H), 7.48 (8H)
B-B[4_n]MCs	−C≡C− frequencies	^{1}H NMR chemical shifts
B-B[4_2]MC	2091	6.85 (4H), 7.31 (2H), 9.14 (2H)
B-B[4_3]MC	2138	7.19 (6H), 7.37 (3H), 7.18 (3H)
B-B[4_4]MC	2152	7.38 (12H), 8.11(4H)
B-B[4_5]MC	2158	7.44 (15H), 7.93 (5H)
B-B[4_6]MC	2160	7.49 (18H), 7.76 (6H)
B-B[4_7]MC[b]	2158	7.41 (7H), 7.56 (14H), 7.73 (7H)
B-B[4_8]MC[c]	2159	7.44 (8H), 7.58 (16H), 7.76 (8H)
B-B[4_8]MC[b]	2160	7.38 (8H), 7.56 (16H), 7.78 (8H)
B-B[4_9]MC[c]		7.41 (9H), 7.55 (18H), 7.77 (9H)
B-B[4_9]MC[b]		7.57 (9H), 7.74 (18H), 7.97 (9H)

[a]Experimental value; $\delta_{scale} = 1.03\delta_{cal} - 1.45$. [b]Boat form. [c]Chair form.

Table 6. The errors observed from the experimental values are 4%, 4.5%, and 4.1% at the B3LYP/6-31G* level of theory. However, when the calculated vibrational frequencies are scaled by a factor of 0.96 for B3LYP/6-31G*[45] (because of overestimation by HF methods), the agreement

SCHEME 4. Homodesmotic Reaction Scheme Containing B-B[4_6]MCs as Reference Molecules

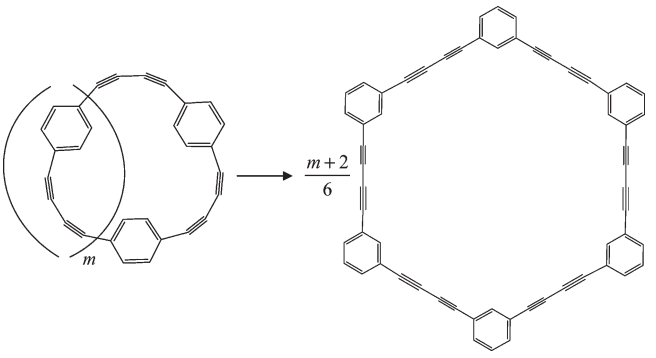

SCHEME 5. Homodesmotic Reaction Scheme for Calculation of the Heats of Formation of (a) B-B[4_n]PCs and (b) 1,4-Di(buta-1,3-diynyl)benzene

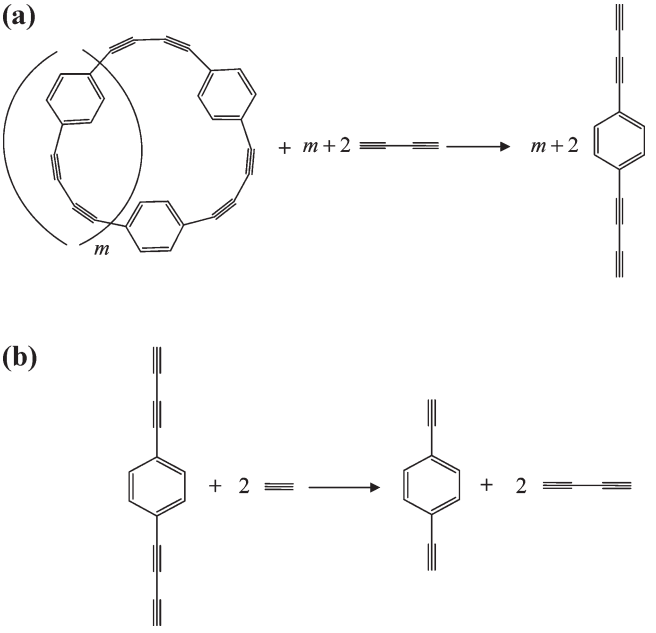

TABLE 7. Scaled Vibrational Frequencies (cm^{-1}), ^{1}H NMR Chemical Shifts (ppm), and Ring Diameters (nm) of B-B[4_n]PCs at the B3LYP/6-31G* Level of Theory

B-B[4_n]PCs	−C≡C− frequencies	^{1}H NMR chemical shifts	ring diameters
B-B[4_2]PC	2073	9.07 (8H)	0.52
B-B[4_3]PC	2119	8.24 (12H)	0.87
B-B[4_4]PC	2132	7.77 (16H)	1.17
B-B[4_5]PC	2165	7.58 (20H)	1.49
B-B[4_6]PC	2192	7.49 (24H)	1.80 (1.50)[a]
B-B[4_7]PC	2195	7.48 (28H)	2.09
B-B[4_8]PC	2200	7.47 (32H)	2.38
B-B[4_9]PC	2213	7.46 (36H)	2.72

[a]Calculated by Ohkita et al. using the PM3 method.

(45) Scott, A. P.; Radom, L. *J. Phys. Chem.* **1996**, *100*, 16502.

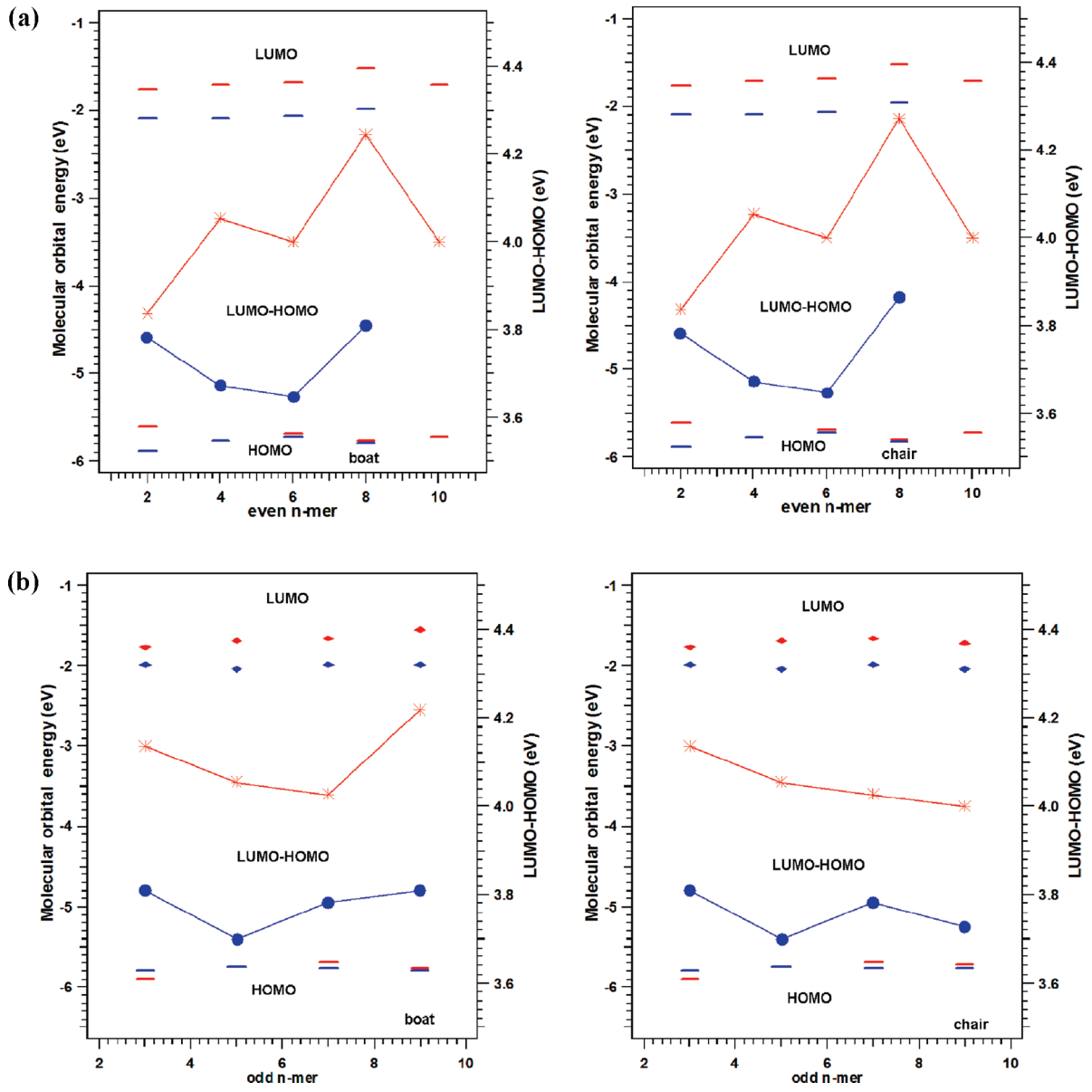

FIGURE 10. HOMO, LUMO, and the LUMO−HOMO gap for (a) even and (b) odd *n* [*n*]CMPAs and B-B[4_n]MCs obtained at the B3LYP/6-31G* level of theory. The red color represents [*n*]CMPAs, and the blue color represents B-B[4_n]MCs.

between the experimental anharmonic and theoretically computed frequencies is very good indeed. We have also used scaled zero-point energy in our calculation.

We have computed ^{1}H NMR chemical shifts of [*n*]CMPAs and B-B[4_n]MCs at B3LYP/6-31G* using the GIAO method[37] with the reference of trimethylsilane (TMS) optimized at the B3LYP/6-31G* level of theory. ^{1}H NMR chemical shifts of [*n*]CMPAs and B-B[4_n]MCs are given in Table 6. Our results, when compared with experimentally measured[5b,c] ^{1}H NMR chemical shifts (ppm) of [3]CMPA and [4]CMPA, have errors in the range of 12−15% between theory and experiment. A linear scaling of ^{1}H NMR chemical shifts of CPAs has been used in order to account for the difference between the experimentally measured and theoretically computed values. For calculation of the linearly scaled values of chemical shifts, we have used $\delta_{scale} = 1.03\delta_{cal} - 1.45$, where δ_{scale} and δ_{cal} are linearly scaled and computed ^{1}H NMR chemical shifts, respectively. Unscaled values of chemical shifts are given in the Supporting Information.

^{1}H NMR chemical shifts of B-B[4_n]PCs were observed, and the singlet indicates that all hydrogen atoms are equivalent. Chemical shift (in ppm) values of B-B[4_2]PC and B-B[4_9]PC are 9.07 and 7.46, respectively. Intermediate values of other B-B[4_n]PCs are given in Table 7. It is clear from Tables 6 and 7 that ^{1}H NMR chemical shift values of [*n*]CMPAs, B-B[4_n]MCs, and B-B[4_n]PCs also correlate well with molecular strain.

3.D. Electronic Properties of [*n*]CMPAs, B-B[4_n]MCs, and B-B[4_n]PCs. HOMO, LUMO, and their spatial distribution for [*n*]CMPAs, B-B[4_n]MCs, and B-B[4_n]PCs are good indicators of many molecular properties such as chemical activity[46] and electronic transport[47−49] and have also been obtained by us at the B3LYP/6-31G* level of theory. Figure 10 shows the HOMO and LUMO levels, as well as their gaps,

for [*n*]CMPAs and B-B[4$_n$]MCs computed using the B3LYP/6-31G* level of theory. The LUMO−HOMO gap of even *n* of [*n*]CMPAs follows a zigzag behavior in both chair and boat forms. In the case of B-B[4$_n$]MCs, the LUMO−HOMO gap decreases first and then increases. An opposite trend was observed in the case of odd *n*. LUMO−HOMO gaps of odd *n* B-B[4$_n$]MCs follow a zigzag behavior, while in the case of odd *n* [*n*]CMPAs, the LUMO−HOMO gap decreases first and then increases. However, in the case of the chair form, it decreases. The HOMOs of [*n*]CMPAs with odd *n* number are doubly degenerate. [*n*]CMPAs show odd−even differences. HOMOs of [*n*]CMPAs with odd *n* are localized, and LUMOs are delocalized except in the case of the boatlike form of [8]CMPA and [9]CMPA, where HOMOs and LUMOs are localized. In the case of B-B[4$_n$]MCs, LUMOs have also been found to be doubly degenerate and LUMOs with odd *n* are localized except in the case of B-B[4$_8$]MC and B-B[4$_9$]MC (for both boat and chair forms). Li et al. have calculated the electronic properties of [*n*]CMPAs (n = 3−10) and B-B[4$_n$]MCs (n = 3−8) using the HF/6-31G* and B3LYP/6-31G* levels of theory.[32,36] Our results with improved geometries also lead to the same conclusion. In our earlier studies,[24] HOMOs of [*n*]CPPAs were found to be doubly degenerate, but not so in the case of B-B[4$_n$]PCs, which may be ascribed to delocalization of the electrons in HOMOs and LUMOs. Spatial distributions of the HOMOs and LUMOs for a series of [*n*]CMPAs (n = 2−10), B-B[4$_n$]MCs, and B-B[4$_n$]PCs (n = 2−9) calculated at the B3LYP/6-31G* level of theory are given in the Supporting Information.

The ring diameters of B-B[4$_2$]PC and B-B[4$_9$]PC are found to be 0.52 and 2.72 nm, respectively. Intermediate values are given in Table 7. Ohkita et al.[16] calculated the ring diameter of B-B[4$_6$]PC as 1.5 nm using the semiempirical (PM3) method. Our calculation on B-B[4$_6$]PC gives a value of 1.8 nm. Ring diameters of B-B[4$_n$]PCs are found to be higher than their [*n*]CPPAs counterparts. The strain energies and heats of formation per unit monomer are inversely proportional to the ring diameter. Ring diameters play an important role in the host−guest chemistry for these kinds of oligomers. Zhao and Truhlar[50] have calculated the interaction energies of guest molecules such as hexamethylbenzene (HMB), fullerene (C_{60} and C_{70}), and three arm-chair-type nanotubes: (3, 3), (4, 4), and (5, 5) with the host molecule [6]CPPAs (HMB@[6]CPPA, C_{60}@[6]CPPA, C_{70}@[6]CPPA, (3,3)@[6]CPPA, (4,4)@[6]-CPPA, and (5,5)@[6]CPPA) using the density functional theory. It would be helpful for experimentalists as well as theoretical researchers to design such types of host−guest systems with host B-B[4$_n$]PCs and guest molecules such as HMB, C_{60},C_{70}, (3,3), (4,4) and (5,5) carbon nanotubes to understand the chemical and electronic properties.

4. Conclusion

Chemically intuitive homodesmotic reaction schemes have been proposed in this paper. Theoretically calculated geometrical parameters of [3]CMPA and [4]CMPA based on these schemes and reported here are in good agreement with the experimentally determined ones wherever the latter is available. Raman frequencies of the −C≡C− bond stretch for [3]CMPA, [4]CMPA, and [6]CMPA are found to have an error margin of 4−4.5% compared to the experimental values, but scaling the theoretical results based on earlier work by other researchers in the field removes most of the discrepancy. Thus, anharmonicity can be accounted for, at least qualitatively. The strain energies of [*n*]CMPAs, B-B[4$_n$]MCs, and B-B[4$_n$]PCs have been calculated using the proposed homodesmotic reaction schemes at B3LYP/6-31G*, mPW1PW91/6-31G*, and M06-2X/6-31+G** levels of theory. For [*n*]CMPAs and B-B[4$_n$]MCs, the strain energy rapidly decreases to zero until [6]CMPA and B-B[4$_6$]MC, increases for [7]CMPA and B-B[4$_7$]MC and chair [8]CMPA and B-B[4$_8$]MC, but decreases subsequently in the case of [9]CMPA, B-B[4$_9$]MC, and [10]-CMPA. It also reaches a plateau that is unlikely to change further. Similar trends have been observed in the case of B-B[4$_n$]PCs. The strain energies of B-B[4$_n$]PCs rapidly decrease as the number of 1-(buta-1,3-diynyl)benzene units increases. The strain energies of B-B[4$_n$]PCs are found to be less when compared to [*n*]CPPAs. In addition, we have also calculated the strain energies for a few lower members of [(2n+2)$_2$] and [(2n+2)$_3$] meta- and paracyclophynes to study the effect of the acetylenic groups in terms of the strain energies. The strain energies have been found to be less if the number of acetylenic groups is more. The experimental heats of formation of these oligomers are unknown. The heats of formation of [*n*]CMPAs, B-B[4$_n$]MCs, and B-B[4$_n$]PCs have also been computed. The heats of formation per unit monomer are directly correlated with the molecular strain. ^{1}H NMR chemical shifts have been obtained using the GIAO method and compared with experimentally available values in the cases of [3]CMPA and [4]CMPA. The errors with respect to experimentally reported values are 12−15% at B3LYP/6-31G*. A linear scaling of computed ^{1}H NMR chemical shifts of CPAs is used to account for differences between the experimentally measured and theoretically computed values. ^{1}H NMR chemical shifts correlate well with the molecular strain of [*n*]CMPAs, B-B[4$_n$]MCs, and B-B[4$_n$]PCs. The ring diameters have been calculated for B-B[4$_n$]PCs. We hope that theoretical calculations of the strain energies and heats of formation, spectroscopic properties (vibrational and NMR), and electronic properties for these oligomers will be helpful in the synthesis, design, and understanding the chemical properties and also in the study of the host−guest chemistry of these macrocycles.

Acknowledgment. M.A.A. thanks the Department of Chemistry, IIT, Madras, for a graduate fellowship for carrying out the research. The authors gratefully acknowledge computational support provided by the High Performance Computing Facility in the Computer Center of IIT, Madras, and Prof. Krishnan Raghavachari, Indiana University, Bloomington, IN, for valuable suggestions. M.A.A. thanks the Supercomputer Education and Research Centre, Indian Institute of Science, Bangalore, India, for use of the M06-2X functional in the *Gaussian 09* program suite. The authors are also grateful to Prof. Daniel A. Singleton, Texas A&M University, College Station, TX,

(46) Fleming, I. *Frontier Molecular Orbitals and Organic Chemical Reactions*; Wiley: London, 1977.
(47) Nitzan, A.; Ratner, M. A. *Science* **2003**, *300*, 1384.
(48) McCreery, R. L. *Chem. Mater.* **2004**, *16*, 4477.
(49) Stokbro, K.; Taylor, J.; Brendyge, M. *J. Am. Chem. Soc.* **2003**, *125*, 3674.
(50) Zhao, Y.; Truhlar, D. G. *J. Am. Chem. Soc.* **2007**, *129*, 8440.

for suggesting the inclusion of single-point strain energy calculations using the M06-2X functional with the 6-31+G** basis set.

Supporting Information Available: Cartesian coordinates, vibrational frequencies, spatial distribution of HOMOs and LUMOs of [*n*]CMPAs, B-B[4_n]MCs, and B-B[4_n]PCs, structures of [$(2n+2)_2$] and [$(2n+2)_3$] meta- and paracyclophynes, and a strain energy plot of CPAs using the mPW1PW91/6-31G* and M06-2X/6-31+G**//B3LYP/6-31G* levels of theory. This material is available free of charge via the Internet at http://pubs.acs.org.